Electronic Supplementary Material (ESI) for ChemComm.
This journal is © The Royal Society of Chemistry 2020

Electronic Supplementary Information (ESI)

Negative Photochromism of a Blue Cyanine Dye

Kazuki Nemoto, Masami Enoki, Ryuzi Katoh,* Katsufumi Suzuki, Tetsuji Murase, Shigeaki Imazeki

Contents

1. Apparatus

The photochromic reaction was induced by photoirradiation with an AM1.5 solar simulator (LAX-C100, Asahi Spectra) at 1 sun intensity. Absorption spectra were measured with an absorption spectrometer (V-670, JUSCO or UV-2450, Shimadzu) fitted with a temperature control attachment (CPS-240A, Shimadzu) to measure temperature-dependence of the temporal change in absorbance.

NMR spectra were measured in DMSO-d_6 on a spectrometer (AL-400, 400 MHz, JEOL) with tetramethylsilane (TMS) as an internal standard. DMSO-d_6 was used as an internal standard ($\delta = 77.0$) in ^{13}C-NMR at 100 MHz. Commercial Merck plates coated with silica gel 60 F-254 were used for analytical thin-layer chromatography, which was visualized by irradiating with UV light. Column chromatography was performed using Wakosil C-200 from FUJIFILM Wako Pure Chemical Corporation, Japan, from which all reagents were obtained.

2. Synthesis

Synthesis of the compounds used in the present study is summarized here. Compound **3** was prepared from compounds **1** and **2** by a reported procedure [L. Yuan, W. Lin, Y. Yang, H. Chen, *J. Am. Chem. Soc.*, 2012, 134, 1200-1211.].

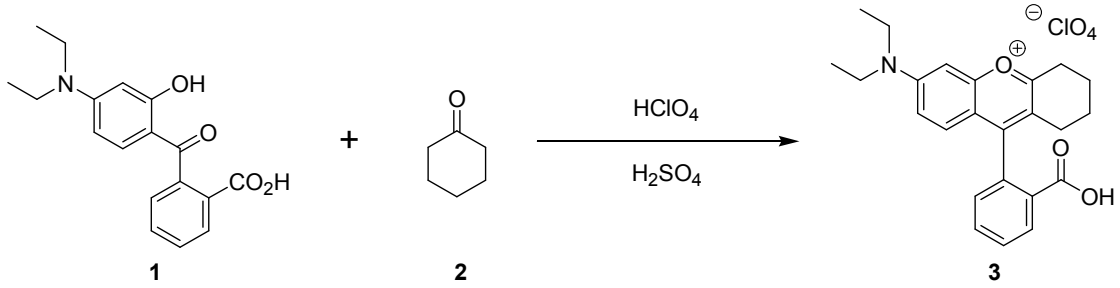

1 2 3

((*E*)-*N*-(9-(2-carboxyphenyl)-5-((9-ethyl-9*H*-carbazol-3-yl)methylene)-5,6,7,8-tetrahydro-3*H*-xanthen-3-ylidene)-*N*-ethylethanaminium tetrakis(pentafluorophenyl)borate (6):

N-ethylcarbazole-3-carboxyaldehyde (**4**) (1.9 g, 8.4 mmol) was added to a solution of **3** (3.8 g, 8.0 mmol) in acetic anhydride (23 mL) at room temperature, and the reaction mixture was heated to 60 °C and stirred for 4 h. After the solvent was removed under vacuum, perchlorate (**5**) was obtained as a black solid. Anion exchange was performed by treating **5** (5.5 g, 8.0 mmol) with lithium tetrakis(pentafluorophenyl)borate (6.1 g, 8.0 mmol) in CH_2Cl_2 (51 mL). After being stirred at room temperature for 2 h, the reaction was quenched by adding water. After separation of the aqueous layer, the organic layer was washed with brine, dried over anhydrous Na_2SO_4, and concentrated to dryness. Purification of the crude mixture by column chromatography (SiO_2, CH_2Cl_2/acetone = 5/1, v/v) gave **6** as a blue solid in 51% yield from **3**. Melting point: 105–108 °C (from CH_2Cl_2/acetone); Rf = 0.6 (CH_2Cl_2/acetone = 5/1); ^{1}H-NMR (400 MHz, CD_2Cl_2) δ 8.43 (1H, s), 8.38 (1H, s), 8.33 (1H, d, J = 8.2 Hz), 8.17 (1H, d, J = 7.8 Hz), 7.82–7.76 (2H, m), 7.72 (1H, td, J = 7.6, 1.2 Hz), 7.59–7.49 (3H, m),

7.33 (1H, t, *J* = 7.3 Hz), 7.20 (1H, d, *J* = 6.9 Hz), 7.07 (1H, d, *J* = 9.6 Hz), 6.98 (1H, d, *J* = 2.7 Hz), 6.96 (1H, s), 4.44 (2H, q, *J* = 7.3 Hz), 3.62 (4H, q, *J* = 7.2 Hz), 3.17 (2H, t, *J* = 6.2 Hz), 2.45 (2H, q, *J* = 5.3 Hz), 1.92–1.86 (2H, m), 1.48 (3H, t, *J* = 7.3 Hz), 1.34 (6H, t, *J* = 7.2 Hz); ^{13}C-NMR (101 MHz, CD_2Cl_2) δ 167.09, 164.01, 163.67, 158.77, 155.58, 150.19–149.56, 147.70–147.16, 141.56, 141.10, 140.53, 140.15–139.73, 138.41–137.64, 135.88–135.21, 135.05, 133.46, 132.11, 130.59, 130.39, 130.13, 130.02, 128.92, 127.13, 126.88, 125.86, 124.51, 123.99, 123.16, 123.07, 120.86, 120.46, 117.35, 117.12, 109.75, 109.59, 95.75, 46.43, 38.36, 27.90, 26.38, 21.84, 13.98, 12.58; FT-IR ν_{max} (ATR, cm^{-1}) 1708, 1630, 1580, 1530, 1512, 1460, 1398, 1380, 1345, 1322, 1262, 1233, 1179, 1150, 1124, 1082, 1024, 975, 920, 819, 774, 755, 709, 683, 660, 608, 573, 536, 496, 424; HRMS (ESI$^+$) calculated for $[M]^+$ *m/z* = 581.2779 ($C_{39}H_{37}N_2O_3$), Found *m/z* = 581.2804

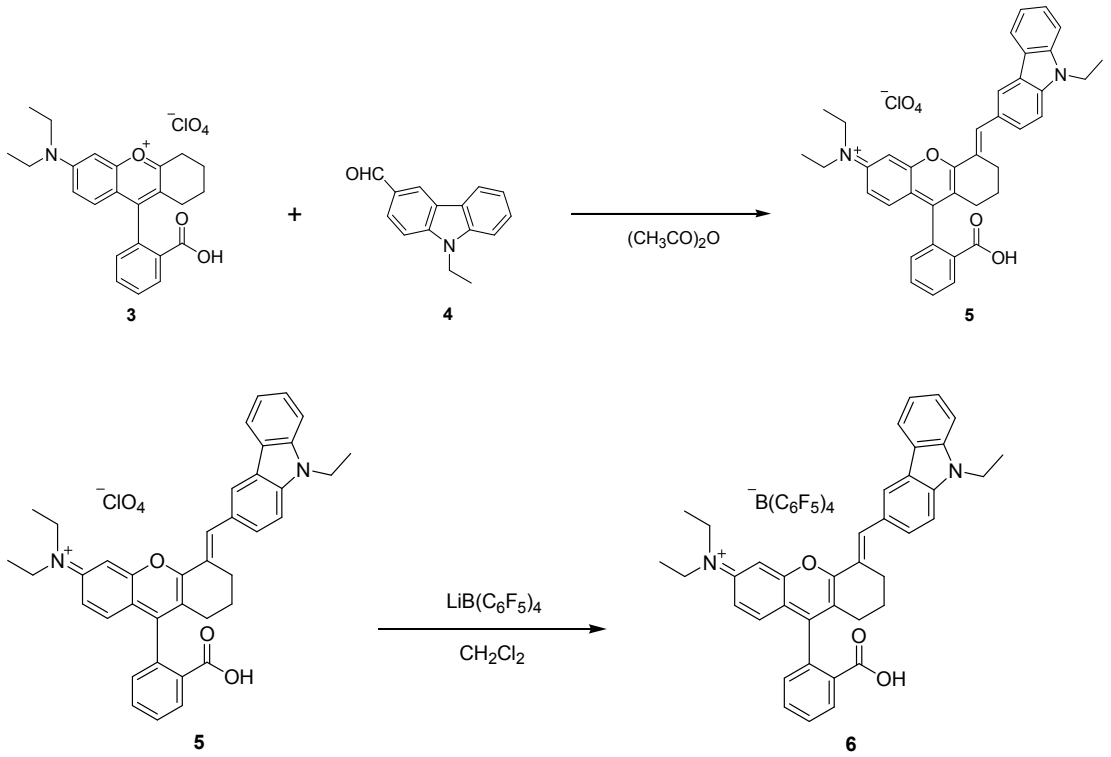

(*E*)-*N*-ethyl-*N*-(5-((9-ethyl-9*H*-carbazol-3-yl)methylene)-9-(2-((2-(methacryloyloxy)ethoxy)carbonyl)phenyl)-5,6,7,8-tetrahydro-3*H*-xanthen-3-ylidene)ethanaminium tetrakis(pentafluorophenyl)borate (<u>8, BCy</u>):

1-Ethyl-3-(3-dimethylaminopropyl)carbodiimide hydrochloride (1.3 g, 6.9 mmol) was added to the solution of **<u>6</u>** (5.1 g, 4.1 mmol), 2-hydroxyethyl methacrylate (**<u>7</u>**) (0.6 g, 4.9 mmol), and 4-dimethylaminopyridine (50 mg, 0.4 mmol) in CH_2Cl_2 (34 mL). After being stirred for 5 h at room temperature, the reaction was quenched by adding water. After separation of the aqueous layer, the organic layer was washed with brine, dried over anhydrous Na_2SO_4, and concentrated to dryness. Purification of the crude mixture by column chromatography (SiO_2, CH_2Cl_2) gave **<u>8</u>** in 21% yield as a

blue solid. Melting point: 110–112 °C (from CH_2Cl_2); Rf = 0.5 (CH_2Cl_2); ^{1}H-NMR (400 MHz, DMSO-d_6) δ 8.58 (1H, s), 8.47 (1H, s), 8.30 (1H, d, *J* = 7.8 Hz), 8.26 (1H, d, *J* = 7.8 Hz), 7.94 (1H, t, *J* = 7.1 Hz), 7.88 (1H, d, *J* = 8.7 Hz), 7.83 (1H, t, *J* = 8.0 Hz), 7.81 (1H, d, *J* = 8.7 Hz), 7.71 (1H, d, *J* = 8.2 Hz), 7.55 (1H, t, *J* = 7.8 Hz), 7.45 (1H, d, *J* = 7.3 Hz), 7.39 (1H, d, *J* = 2.3 Hz), 7.31 (1H, t, *J* = 7.8 Hz), 7.27 (1H, dd, *J* = 10.1, 2.3 Hz), 6.98 (1H, d, *J* = 9.6 Hz), 5.88 (1H, s), 5.62 (1H, s), 4.53 (2H, q, *J* = 7.3 Hz), 4.39 (2H, d, *J* = 4.1 Hz), 4.15 (2H, d, *J* = 4.1 Hz), 3.70 (4H, q, *J* = 7.2 Hz), 3.12 (2H, t, *J* = 6.0 Hz), 2.40–2.31 (2H, m), 1.88–1.73 (2H, m), 1.79 (3H, s), 1.38 (3H, t, *J* = 7.3 Hz), 1.27 (6H, t, *J* = 7.2 Hz); ^{13}C-NMR (101 MHz, DMSO-d_6) δ 166.73, 165.23, 162.89, 161.42, 158.42, 155.61, 149.49–148.92, 147.22–146.56, 141.04, 140.75, 139.69, 139.69–139.12, 137.66–136.58, 135.84, 135.21–134.68, 134.68, 134.18, 131.50, 130.84, 130.11, 129.89, 129.77, 128.66, 127.09, 126.91, 126.48, 125.96, 124.63, 123.35, 122.78, 122.39, 121.24, 120.33, 118.38, 117.20, 110.27, 110.16, 96.15, 63.79, 62.94, 45.90, 37.84, 27.30, 26.01, 21.57, 18.31, 14.23, 12.96; FT-IR ν_{max} (ATR, cm^{-1}) 1720, 1629, 1579, 1530, 1512, 1460, 1433, 1397, 1378, 1344, 1321, 1260, 1232, 1177, 1149, 1123, 1081, 975, 919, 812, 769, 754, 708, 683, 660, 604, 573, 535, 495, 422; HRMS (ESI$^+$) calculated for $[M]^+$ *m/z* = 693.3323 ($C_{45}H_{45}N_2O_5$), Found *m/z* = 693.3328

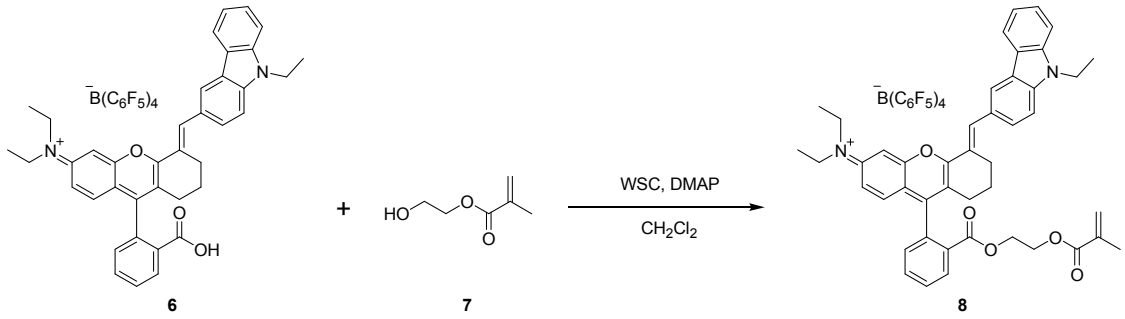

6 **7** **8**

^{1}H-NMR of 6 (CD_2Cl_2)

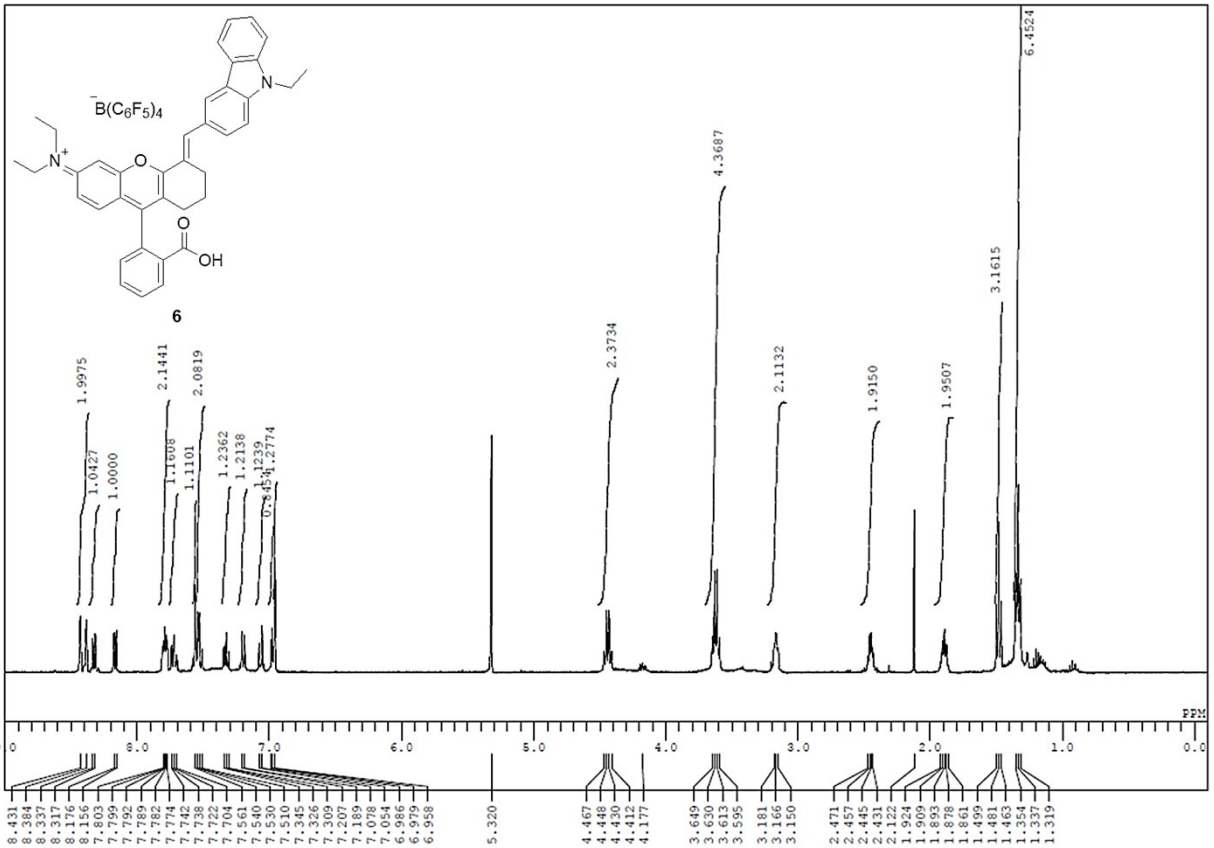

^{13}C-NMR of 6 (CD_2Cl_2)

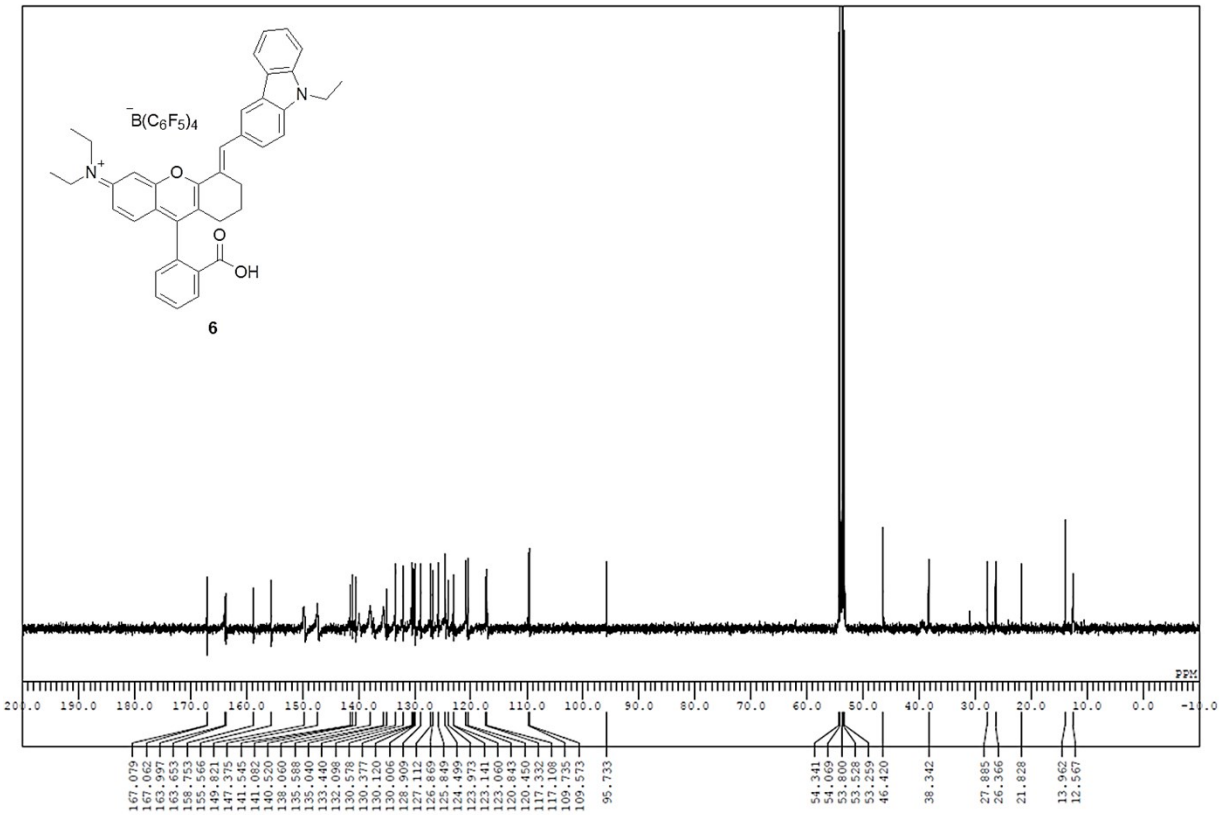

^{1}H-NMR of 8 (DMSO-d_6)

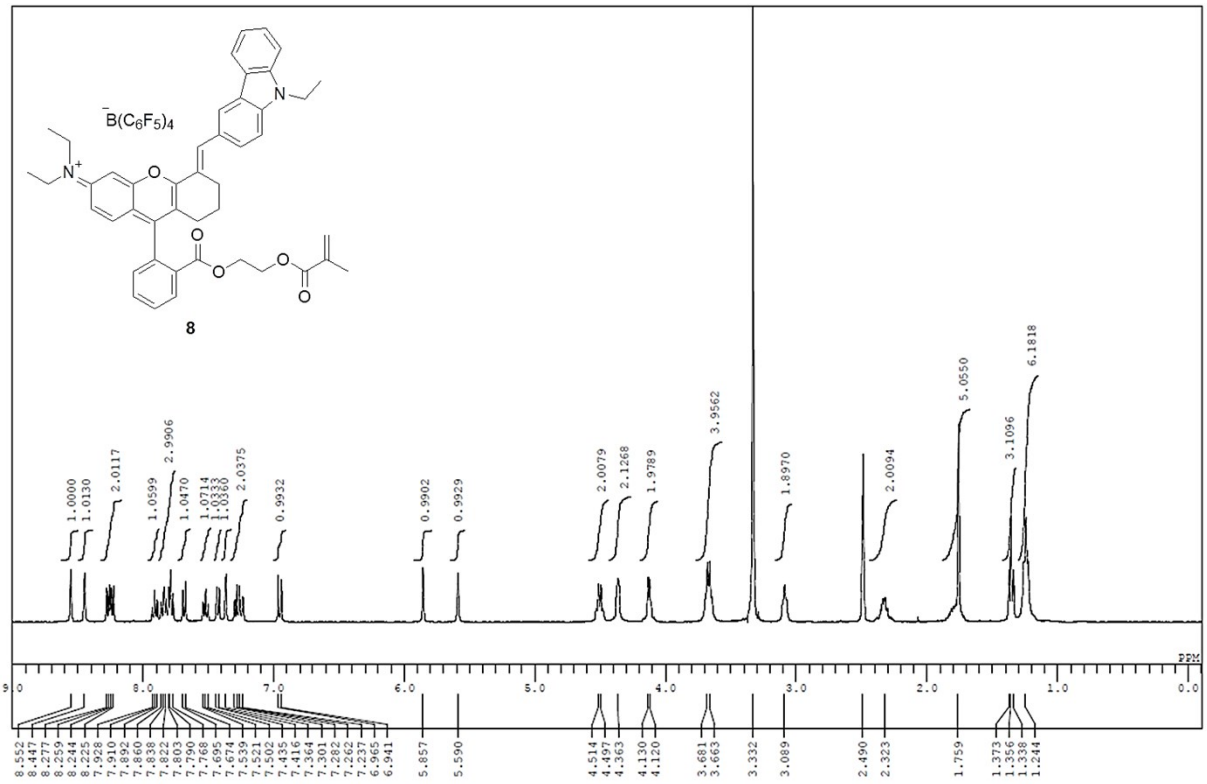

^{13}C-NMR of 8 (DMSO-d_6)

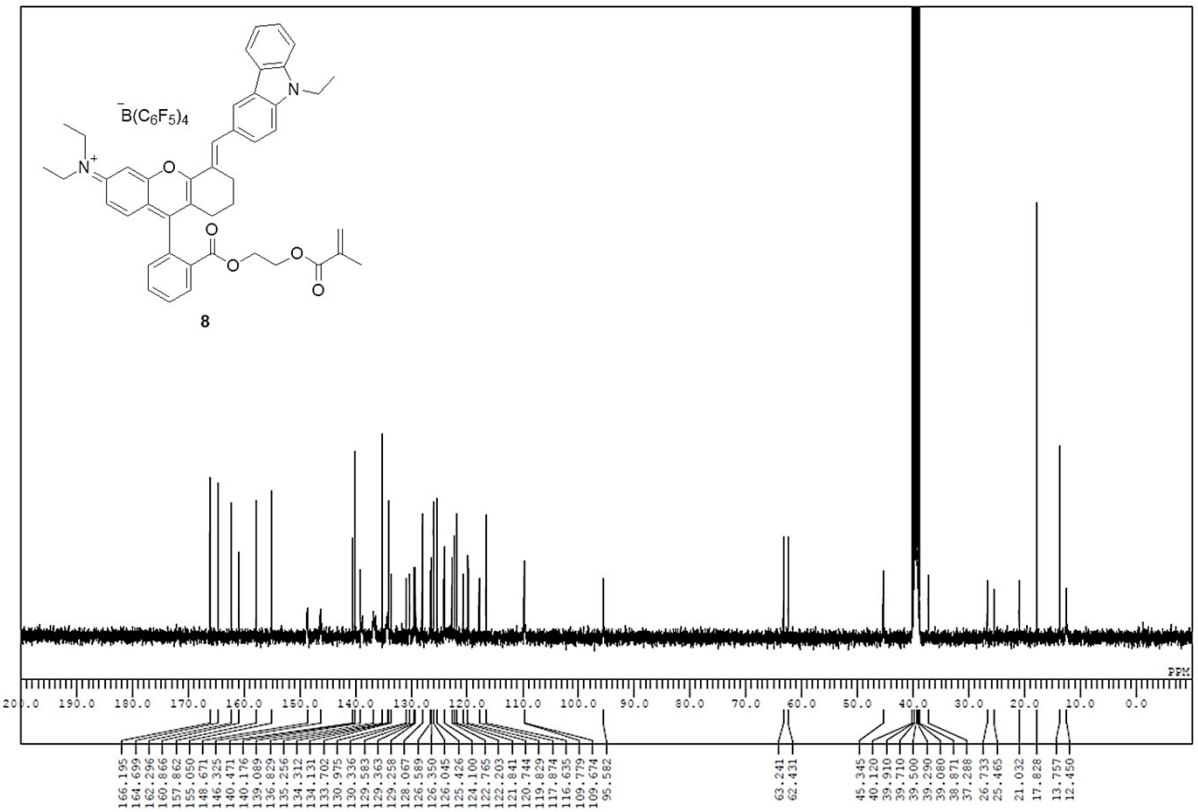

3. Recovery time at room temperature

The temporal change in recovery after light irradiation (AM1.5, 1 sun) at room temperature for BCy in toluene (1.8 x 10^{-5} M) observed at 650 nm is shown in Fig. S1. A_0 denotes the absorbance just after light irradiation. The data (A_0 - A) can be fitted by a single exponential function and thus the time constant τ_R of the recovery reaction was evaluated to be 100 min.

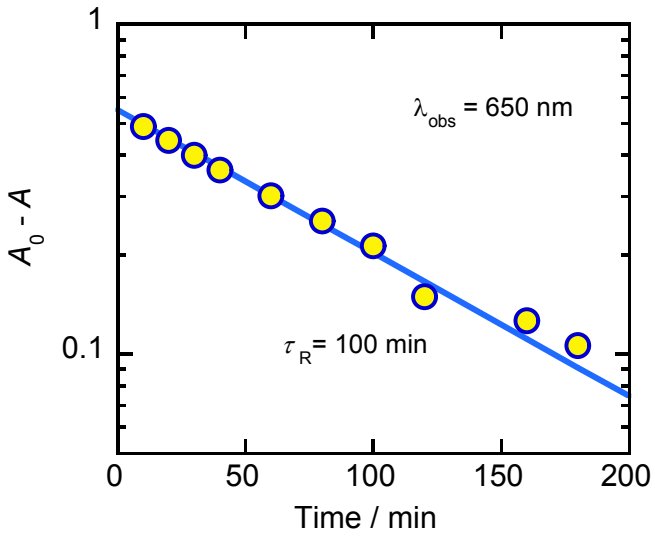

Fig. S1 Temporal change in recovery after light irradiation for BCy in toluene observed at 650 nm at room temperature.

4. Photochromic reaction of BCy in polar solvents

In some other solvents, similar photochromic behavior was observed. Fig. S2 shows the temporal change in recovery after light irradiation (AM1.5, 1 sun) at room temperature for BCy in toluene (Tol), 2-propernol (2PrOH), methanol (MeOH) and acetonitrile (MeCN) observed at 650 nm. Time constant of the recovery reaction was estimated to be 100 min for Tol, 85 min for 2PrOH, 45 min for MeOH and 35 min for MeCN. It is noted that the deviation form a single exponential function was observed at longer time range for MeOH and MeCN. This suggests that degradation of BCy occurs in MeOH and MeCN.

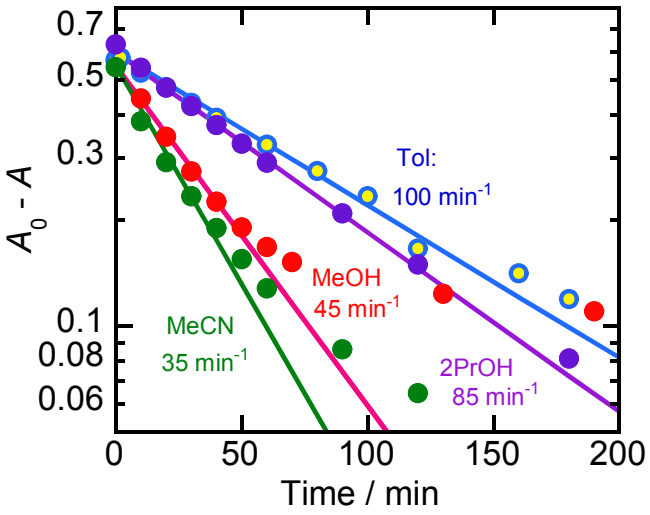

Fig. S2 Temporal change in recovery after light irradiation for BCy in toluene (tol), 2-propernol (2PrOH), methanol (MeOH) and acetonitrile (MeCN) observed at 650 nm at room temperature.

5. DFT calculation

DFT calculations of molecular structures and absorption spectra were performed using the Gaussian 09 program based on B3LYP/6-31G(d) level. To reduce calculation time, the derivative of BCy shown in Scheme S1 was used instead of the original BCy. Figure S3 shows clearly that the absorption coefficient (epsilon) of the *E*-form is sufficiently higher than that of the *Z*-form, which is consistent with the experimental results. The detail of the excitation energies and oscillator strengths of E- and Z- forms are listed in Tables S1 and S2, respectively. As the optimized structures of the *E*- and *Z*-forms of BCy in Fig. S4 show, the *E*-form is a planar structure; specifically, two chromophores (green and pink parts) are in the same plane. In contrast, the *Z*-form is a non-planar structure. Clearly, the difference in planarity leads to the large difference in absorption coefficient.

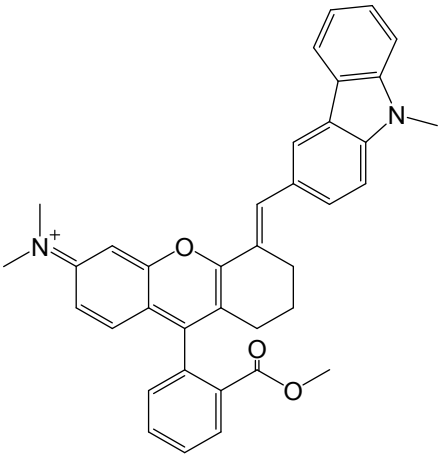

Scheme S1 Molecular structure of the derivative of BCy for DFT calculation

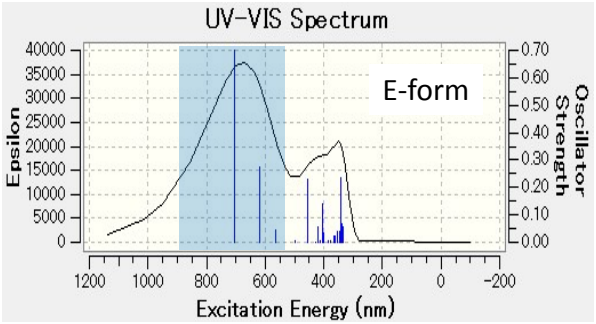

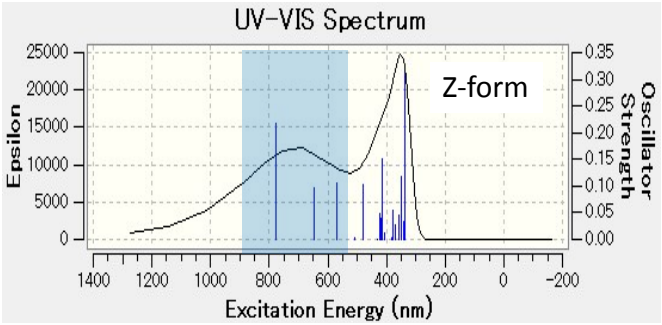

Fig. S3 Absorption spectra of the *E*-form and *Z*-form obtained by TD-DFT calculation.

Table S1 Calculated excitation energies and oscillator strengths of *E*-form

Excited State	1:	Singlet-A	1.7634 eV	703.08 nm	f=0.6992	<S**2>=0.000
144 ->147		0.13740				
145 ->147		0.24017				
146 ->147		0.64417				

This state for optimization and/or second-order correction.

Total Energy, E(TD-HF/TD-KS) = -1764.09472411

Copying the excited state density for this state as the 1-particle RhoCI density.

Excited State	2:	Singlet-A	2.0042 eV	618.62 nm	f=0.2735	<S**2>=0.000
144 ->147		0.41819				
145 ->147		0.49325				
146 ->147		-0.26550				
Excited State	3:	Singlet-A	2.1988 eV	563.87 nm	f=0.0470	<S**2>=0.000
144 ->147		0.53507				
145 ->147		-0.41819				
146 ->149		0.13868				
Excited State	4:	Singlet-A	2.4813 eV	499.68 nm	f=0.0046	<S**2>=0.000
146 ->148		0.70401				
Excited State	5:	Singlet-A	2.7125 eV	457.08 nm	f=0.2322	<S**2>=0.000
143 ->147		0.66266				
146 ->147		-0.11578				
146 ->149		0.10825				
Excited State	6:	Singlet-A	2.8955 eV	428.20 nm	f=0.0018	<S**2>=0.000
145 ->148		0.70457				
Excited State	7:	Singlet-A	2.9649 eV	418.18 nm	f=0.0546	<S**2>=0.000
142 ->147		0.68695				
Excited State	8:	Singlet-A	3.0155 eV	411.15 nm	f=0.0042	<S**2>=0.000
141 ->147		0.69569				

Excited State 9:	Singlet-A	3.0590 eV	405.30 nm	f=0.1403	<S**2>=0.000
139 ->147	0.14884				
140 ->147	0.32875				
144 ->148	0.18899				
145 ->149	0.19271				
146 ->149	0.52029				
Excited State 10:	Singlet-A	3.0742 eV	403.30 nm	f=0.0087	<S**2>=0.000
140 ->147	-0.17150				
144 ->148	0.67304				
146 ->149	-0.10857				
Excited State 11:	Singlet-A	3.0950 eV	400.60 nm	f=0.0338	<S**2>=0.000
139 ->147	-0.35103				
140 ->147	0.54759				
145 ->149	-0.11527				
146 ->149	-0.20944				
Excited State 12:	Singlet-A	3.2354 eV	383.21 nm	f=0.0029	<S**2>=0.000
144 ->149	-0.13804				
145 ->149	-0.27906				
145 ->150	-0.13550				
146 ->150	0.60201				
Excited State 13:	Singlet-A	3.3022 eV	375.46 nm	f=0.0046	<S**2>=0.000
138 ->147	-0.12622				
139 ->147	0.51239				
140 ->147	0.19543				
145 ->149	-0.28528				
146 ->149	-0.13715				
146 ->150	-0.17321				
146 ->151	0.12690				
Excited State 14:	Singlet-A	3.3871 eV	366.04 nm	f=0.0233	<S**2>=0.000
138 ->147	0.27071				
145 ->149	0.23120				
146 ->150	0.10571				
146 ->151	0.58093				

Excited State 15:	Singlet-A	3.4322 eV	361.24 nm	f=0.0248	<S**2>=0.000
137 ->147	-0.21662				
138 ->147	0.48974				
139 ->147	0.16747				
145 ->149	0.10943				
145 ->150	-0.11540				
146 ->149	-0.13048				
146 ->151	-0.33077				
146 ->152	-0.10507				
Excited State 16:	Singlet-A	3.4952 eV	354.72 nm	f=0.0413	<S**2>=0.000
137 ->147	-0.14185				
138 ->147	-0.14613				
144 ->149	0.61768				
145 ->150	-0.22904				
Excited State 17:	Singlet-A	3.5939 eV	344.99 nm	f=0.0392	<S**2>=0.000
138 ->147	0.10119				
143 ->148	0.65303				
145 ->149	-0.15914				
Excited State 18:	Singlet-A	3.6228 eV	342.23 nm	f=0.2336	<S**2>=0.000
137 ->147	0.35360				
138 ->147	-0.14671				
139 ->147	0.14829				
143 ->148	0.24184				
145 ->149	0.30919				
146 ->149	-0.19689				
146 ->150	0.15431				
146 ->152	-0.19174				
146 ->153	-0.12070				
Excited State 19:	Singlet-A	3.6525 eV	339.45 nm	f=0.0667	<S**2>=0.000
137 ->147	-0.33999				
144 ->150	-0.16335				
145 ->150	0.53120				
146 ->150	0.16865				

Excited State 20:	Singlet-A	3.6906 eV	335.94 nm	f=0.0584	<S**2>=0.000
137 ->147	-0.20001				
138 ->147	-0.16597				
144 ->149	-0.13675				
145 ->149	0.16317				
145 ->150	-0.10631				
145 ->151	-0.13494				
146 ->149	-0.11124				
146 ->152	0.52270				
146 ->153	-0.12982				

Table S2 Calculated excitation energies and oscillator strengths of *Z*-form

Excited State 1:	Singlet-A	1.5990 eV	775.37 nm	f=0.2164	<S**2>=0.000
145 ->147	0.19777				
146 ->147	0.66963				

This state for optimization and/or second-order correction.

Total Energy, E(TD-HF/TD-KS) = -1764.09253050

Copying the excited state density for this state as the 1-particle RhoCI density.

Excited State 2:	Singlet-A	1.9165 eV	646.93 nm	f=0.0977	<S**2>=0.000
144 ->147	-0.41422				
145 ->147	0.52891				
146 ->147	-0.19996				
Excited State 3:	Singlet-A	2.1792 eV	568.93 nm	f=0.1058	<S**2>=0.000
144 ->147	0.54704				
145 ->147	0.40024				
146 ->149	-0.14157				
Excited State 4:	Singlet-A	2.4443 eV	507.24 nm	f=0.0020	<S**2>=0.000
146 ->148	0.70328				
Excited State 5:	Singlet-A	2.5885 eV	478.98 nm	f=0.1018	<S**2>=0.000
143 ->147	0.67387				

Excited State 6:	Singlet-A	2.8713 eV	431.80 nm	f=0.0005	<S**2>=0.000	
145 ->148	0.70529					
Excited State 7:	Singlet-A	2.9426 eV	421.34 nm	f=0.0493	<S**2>=0.000	
142 ->147	0.67927					
Excited State 8:	Singlet-A	2.9730 eV	417.03 nm	f=0.0402	<S**2>=0.000	
141 ->147	0.63851					
146 ->149	-0.26531					
Excited State 9:	Singlet-A	2.9896 eV	414.72 nm	f=0.1505	<S**2>=0.000	
139 ->147	0.13884					
140 ->147	0.23563					
141 ->147	0.27406					
145 ->149	0.21052					
146 ->149	0.52791					
Excited State 10:	Singlet-A	3.0504 eV	406.45 nm	f=0.0109	<S**2>=0.000	
139 ->147	-0.34747					
140 ->147	0.56686					
144 ->148	-0.19180					
Excited State 11:	Singlet-A	3.0566 eV	405.63 nm	f=0.0039	<S**2>=0.000	
139 ->147	-0.12234					
140 ->147	0.13893					
144 ->148	0.67683					
Excited State 12:	Singlet-A	3.2392 eV	382.76 nm	f=0.0021	<S**2>=0.000	
139 ->147	0.34969					
140 ->147	0.16708					
144 ->149	0.15357					
145 ->149	-0.34068					
146 ->150	0.41373					
Excited State 13:	Singlet-A	3.2858 eV	377.34 nm	f=0.0541	<S**2>=0.000	
137 ->147	0.11748					
139 ->147	-0.40658					
140 ->147	-0.21360					
144 ->149	0.15233					

146 ->149	0.14801				
146 ->150	0.42340				
Excited State 14:	Singlet-A	3.3367 eV	371.57 nm	f=0.0270	<S**2>=0.000
137 ->147	0.12057				
138 ->147	0.45350				
145 ->149	-0.28389				
146 ->150	-0.19102				
146 ->151	-0.37623				
Excited State 15:	Singlet-A	3.3669 eV	368.24 nm	f=0.0176	<S**2>=0.000
137 ->147	0.15958				
138 ->147	0.33623				
146 ->151	0.56041				
146 ->152	0.12425				
Excited State 16:	Singlet-A	3.4546 eV	358.90 nm	f=0.0454	<S**2>=0.000
137 ->147	0.13336				
138 ->147	-0.19885				
144 ->149	0.56824				
145 ->149	-0.14012				
145 ->150	0.16675				
146 ->150	-0.20971				
Excited State 17:	Singlet-A	3.5408 eV	350.16 nm	f=0.0193	<S**2>=0.000
137 ->147	0.13342				
143 ->148	0.67000				
145 ->149	0.10694				
Excited State 18:	Singlet-A	3.5441 eV	349.83 nm	f=0.1175	<S**2>=0.000
137 ->147	0.49551				
139 ->147	0.11338				
143 ->148	-0.20242				
145 ->149	0.21292				
146 ->149	-0.12057				
146 ->152	-0.30751				
Excited State 19:	Singlet-A	3.6142 eV	343.04 nm	f=0.0346	<S**2>=0.000

137 ->147	0.25421					
144 ->150	-0.11843					
145 ->150	-0.42219					
146 ->152	0.44108					

Excited State 20:	Singlet-A	3.6688 eV	337.94 nm	f=0.3227	<S**2>=0.000
137 ->147	-0.16669				
138 ->147	0.22300				
144 ->149	0.16693				
144 ->150	0.14436				
145 ->149	0.29772				
145 ->150	0.23532				
146 ->149	-0.15395				
146 ->150	0.13179				
146 ->152	0.29523				
146 ->153	-0.14763				

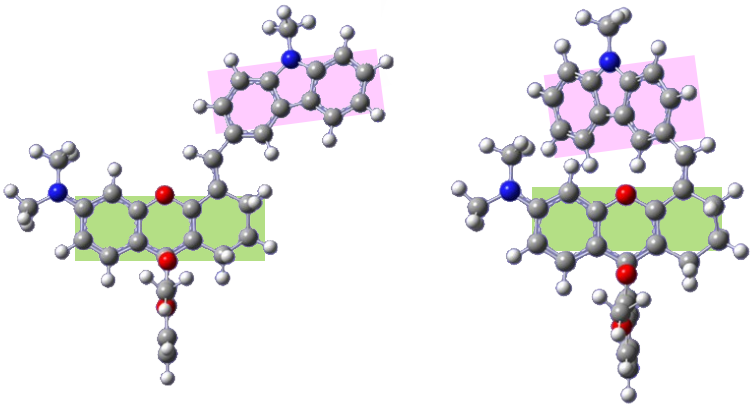

E-form Z-form

Total energy (a.u.)		Δ_{E-Z}
***E*-form**	***Z*-form**	**(kcal/mol)**
-1764.92452	-1764.83092	58.7

Fig. S4 Optimized structures of the *E*-form and *Z*-form obtained by DFT calculation.

6. NMR study on the molecular structure of BCy before and after light irradiation

Molecular structure change of BCy induced by light irradiation was studied by NMR. Fig. S5 shows key ROESY correlations of BCy in DMSO-d_6 under dark condition. The correlation peaks (red circles) were clearly observed. This indicates that BCy before light irradiation is E-form. In order to study photo-induced conformation change of E-form of BCy, ^{1}H-NMR spectra of BCy in CD_3OD were measured before and after light irradiation (Fig. S6). Large shift of Ha indicates significant change of the anisotropy effect from carbazole moiety. This suggests isomerization from E-form to Z-form occurs by light irradiation.

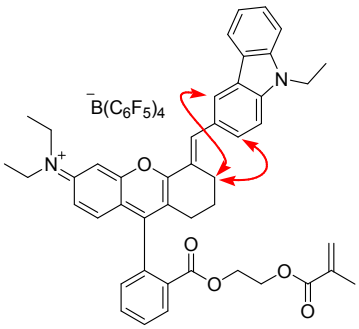

8

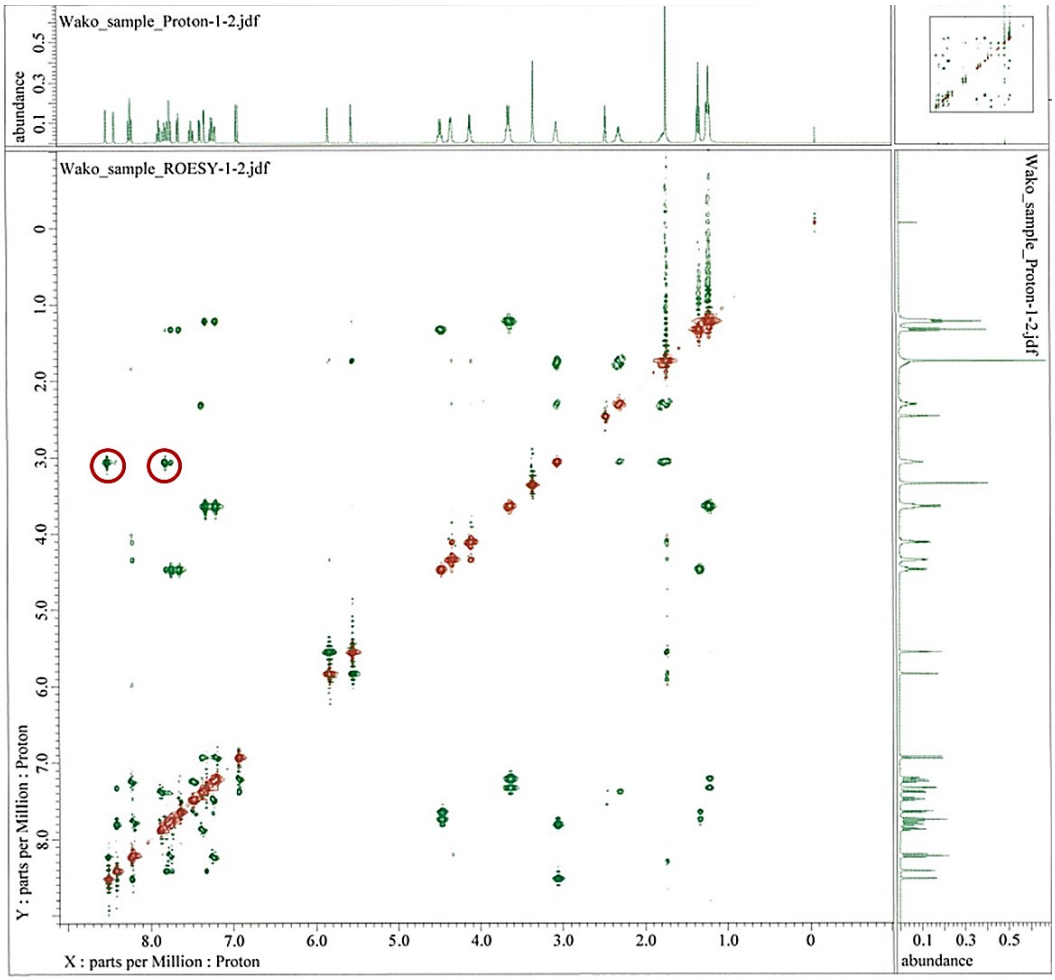

Fig. S5 Key ROSSY correlations of BCy in DMSO-d_6.

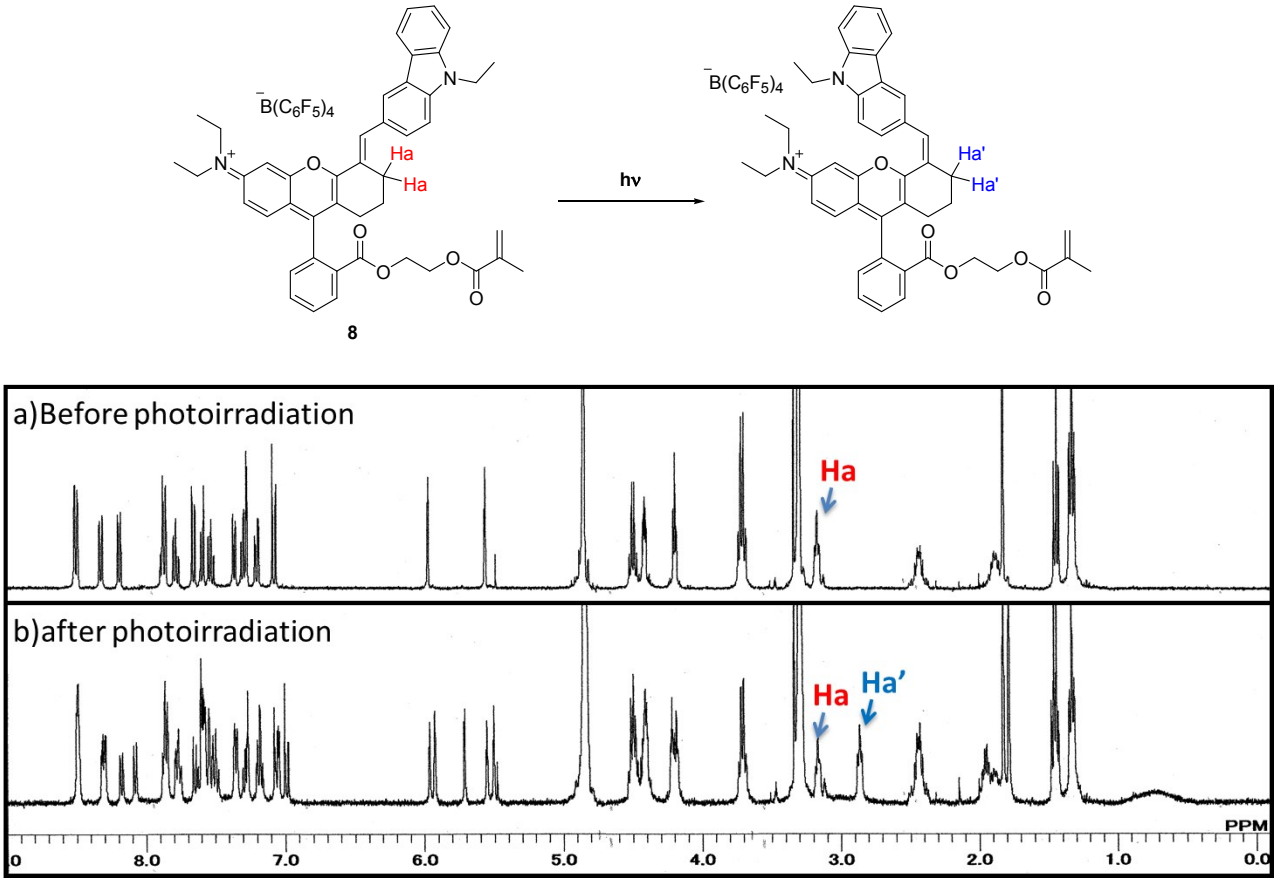

Fig. S6 ^{1}H-NMR spectra of BCy in CD_3OD before and after light irradiation.

7. Quantum yield of the photochromic reaction of BCy in toluene

Absorption spectra of BCy in toluene under photostationary state (Fig. 1) were divided into two components of E- and Z-forms based on the similarity with the spectra obtained in acetonitrile shown in Fig. 2b. Fig. S7 shows the absorption spectra of E- and Z-forms of BCy in toluene. From this, the ratio of E/Z forms of BCy in toluene was estimated to be 0.24 in photostatinary state under AM1.5 (1 sun) irradiation condition shown in Fig. 1a.

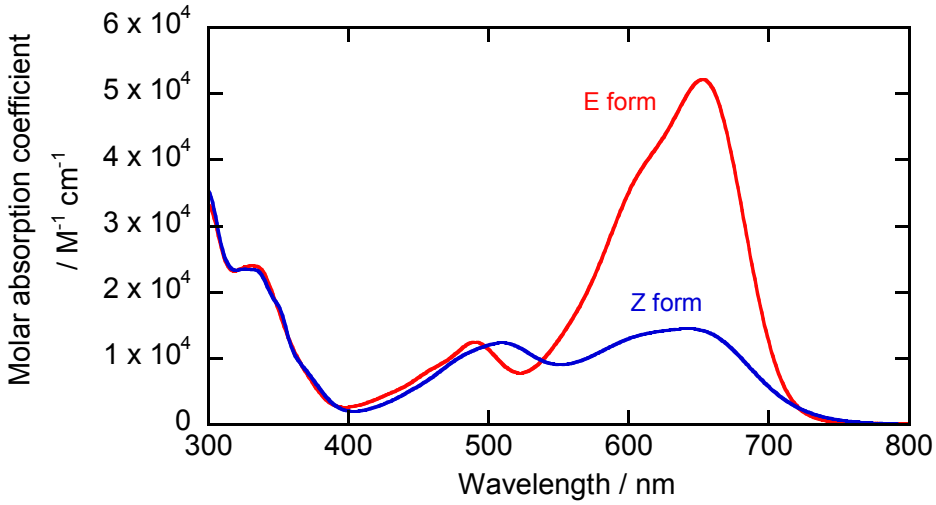

Fig. S7 Absorption spectra of E-form and Z-form of BCy in toluene

In order to estimate the quantum yield of the forward (E→Z) and the recovery (Z→E) reactions, the temporal change of absorbance during light irradiation at room temperature was observed at 633 nm (Fig. S8). Excitation was carried out at 633 nm using He-Ne laser (JDSU, 1125P, 5 mW). After light irradiation for several seconds, absorbance at 633 nm was immediately measured with an absorption spectrometer (V-670, JUSCO). As shown in Fig. S8, the absorbance decreases with time and then becomes constant. This clearly indicates that the reaction reaches to the photostationary state.

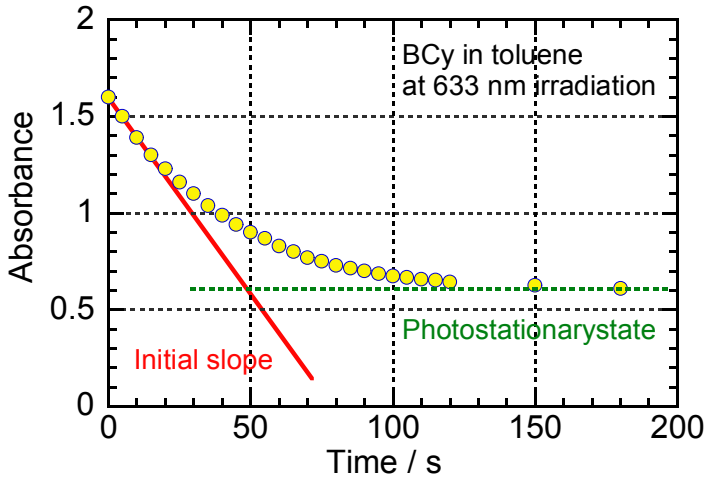

Fig. S8 Temporal change of absorbance observed at 633 nm during light irradiation at 633 nm of BCy in toluene at room temperature.

Temporal change of the concentration [E] of E-form can be expresses as

$$\frac{d[\mathrm{E}]}{dt} = -N_{\mathrm{photon}}^{\mathrm{abs}} \frac{A_E}{A_{\mathrm{obs}}} \Phi_{\mathrm{E}\to\mathrm{Z}} + N_{\mathrm{photon}}^{\mathrm{abs}} \frac{A_Z}{A_{\mathrm{obs}}} \Phi_{Z\to E} - k_T \left([\mathrm{E}_0] - [\mathrm{E}]\right) \qquad \text{(eq. S1)}$$

where $N_{\mathrm{photon}}{}^{\mathrm{abs}}$ is the concentration of the absorbed photon per unit time in the sample solution, $[\mathrm{E}_0]$ is the initial concentration of E, A_{E} and A_{Z} is the absorbance due to E-form and Z-form, respectively and $\Phi_{\mathrm{E}\to\mathrm{Z}}$ and $\Phi_{\mathrm{Z}\to\mathrm{E}}$ is the quantum yield of E→Z and Z→E reactions, respectively and k_{T} is the rate constant of the thermal recovery reaction. In the present case, the third term in the right hand side of eq. S1 can be ignored because the thermal recovery reaction (Fig. S1) is much slower than the temporal change observed shown in Fig. S8.

At the initial stage of light irradiation, [E] equals $[\mathrm{E}_0]$ and thus the second term can be neglected. Hence, $\Phi_{\mathrm{E}\to\mathrm{Z}}$ could be estimated to be 0.046 from the initial slope shown in Fig. S8 using the values of the volume of the sample solution (2.9 mL) the light intensity (5 mW) and absorbance (1.6) at the excitation wavelength (633 nm).

After sufficient light irradiation time, the absorbance reaches photostationary state. At the condition, eq. S1 can be solved as

$$\Phi_{Z\to E} = \frac{\varepsilon_{\mathrm{E}}}{\varepsilon_{\mathrm{Z}}} \frac{[\mathrm{E}]}{[Z]} \Phi_{\mathrm{E}\to\mathrm{Z}} \qquad \text{(eq. S2)}$$

where ε_{E} and ε_{Z} are the molar absorption coefficients of E- and Z-forms at the observed wavelength

(633 nm), respectively. Hence, $\Phi_{Z\rightarrow E}$ could be estimated to be 0.015 using the values of ε_E = 4.6 x 10^4 $M^{-1}cm^{-1}$ and ε_Z = 1.4 x 10^4 $M^{-1}cm^{-1}$ at 633 nm (Fig. S7), the relative ratio [E]/[Z] = 0.1 obtained from the analysis of the absorption spectra.

8. Temperature dependence of the recovery time

The temporal change in recovery after light irradiation for BCy in toluene observed at 650 nm used for the Arrhenius plot (Fig. 3) is shown in Figure S9.

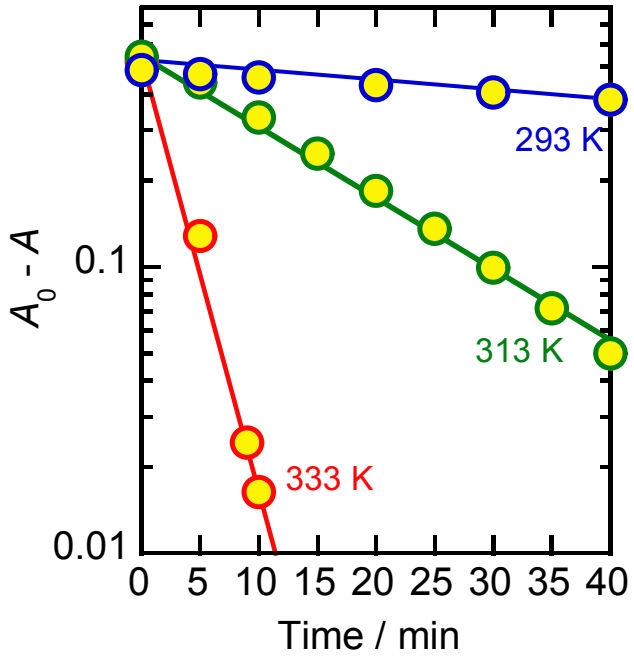

Fig. S9 Temporal change in recovery after light irradiation for BCy in toluene observed at 650 nm at various temperatures.